



## Sub-millennial climate variability from high resolution water isotopes in the EDC ice core

Antoine Grisart<sup>(1)</sup>, Mathieu Casado<sup>(1,3)</sup>, Vasileios Gkinis<sup>(2)</sup>, Bo Vinther<sup>(2)</sup>, Philippe Naveau<sup>(1)</sup>, Mathieu Vrac<sup>(1)</sup>, Thomas Laepple<sup>(3)</sup>, Bénédicte Minster<sup>(1)</sup>, Frederic Prié<sup>(1)</sup>, Barbara Stenni<sup>(4)</sup>, Elise Fourré<sup>(1)</sup>, Hans-Christian Steen Larsen<sup>(5)</sup>, Jean Jouzel<sup>(1)</sup>, Martin Werner<sup>(6)</sup>, Katy Pol<sup>(1)</sup>, Valérie Masson-Delmotte<sup>(1)</sup>, Maria Hoerhold<sup>(6)</sup>, Trevor Popp<sup>(2)</sup>, Amaelle Landais<sup>(1)</sup>

<sup>1</sup> Laboratoire des Sciences du Climat et de l'Environnement, CEA–CNRS–UVSQ–Paris-Saclay–IPSL, Gif-sur-Yvette, France

<sup>2</sup> Physics of Ice, Climate and Earth, Niels Bohr Institute, University of Copenhagen, Copenhagen, Denmark

<sup>3</sup> Alfred Wegener Institute, Helmholtz Center for Polar and Marine Research, Potsdam, Germany

<sup>4</sup> Department of Environmental Sciences, Informatics and Statistics, University Ca' Foscari of Venice, Venice, Italy

<sup>5</sup> Geophysical Institute, University of Bergen and Bjerknes Centre for Climate Research, Bergen 5020, Norway

<sup>6</sup> Alfred Wegener Institute, Helmholtz Centre for Polar and Marine Research, Bremerhaven, Germany

*Correspondence to:* Antoine Grisart (antoine.grisart@lscce.ipsl.fr)

**Abstract.** The EPICA Dome C (EDC) ice core provides the longest continuous climatic record covering the last 800 000 years (800 kyrs). Obtaining homogeneous high resolution measurements and accounting for diffusion provide a unique opportunity to study decadal to millennial variability within the past glacial and interglacial periods. We present here a compilation of high resolution (11 cm) water isotopic records with 27,000  $\delta^{18}\text{O}$  measurements and 7,920  $\delta\text{D}$  measurements (covering respectively 94 % and 27 % of the whole EDC record), including both published and new measurements (2,900 for both  $\delta^{18}\text{O}$  and  $\delta\text{D}$ ) over the last 800 kyrs on the EDC ice core. We show that overlapping time series performed over multiple depth ranges over the past 20 years, using different analytical methods and in different laboratories, are consistent within analytical uncertainty, and therefore can be combined to provide a homogeneous data set. A frequency decomposition of the most complete  $\delta^{18}\text{O}$  record and a simple assessment of the possible influence of diffusion on the measured profile shows that the variability during glacial periods at multi-decadal to multi-centennial timescale is higher than variability of the interglacial periods. This analysis shows as well that during interglacial periods characterized by a temperature optimum at its beginning, the multi-centennial variability is the strongest over this temperature optimum.

### 1 Introduction

Water isotopes in ice cores ( $\delta^{18}\text{O}$ ,  $\delta\text{D}$ ) are valuable tools to reconstruct past temperatures in polar regions. Along air mass transportation, distillation of moisture from the low latitude regions of evaporation to the polar regions leads to a loss of heavy isotopes during successive precipitation events and hence to a decrease of  $\delta^{18}\text{O}$  and  $\delta\text{D}$  toward cold regions. Despite known limitations due to temporal changes in intermittency of precipitation (Casado et al., 2020), vapor origin and transport (Helsen et al., 2006), sea ice extent (Noone, 2004), changes in condensation vs surface temperatures (Buizert et al., 2021) or deposition and post-deposition effects (Casado et al., 2018), the spatial relationship between surface temperature and surface snow  $\delta\text{D}$



and  $\delta^{18}O$  has long been used to establish an isotopic paleothermometer to infer past temperature variations at least qualitatively (Jouzel et al., 2013).

35 Today, the oldest continuous isotopic record from ice cores has been retrieved at the Dome C through the European Project for Ice Coring Antarctica (EPICA) Dome C ice core (EDC) covering the last 800,000 years (800 kyrs) (Jouzel et al., 2007). The first analyses of water isotopic composition ( $\delta D$ ) over the EDC ice core were displayed at a  $\sim 4$  m resolution providing the first picture of the succession of the 8 glacial – interglacial cycles (EPICA community members, 2004). Several years later, systematic measurements of  $\delta D$  on bag samples (55 cm) evidenced the millennial scale variability over the glacial periods in  
40 Antarctica (Jouzel et al., 2007; Stenni et al., 2010). In the following years, some studies focused on even higher resolution (11 cm) on some key periods to study the high frequency climate variability. In order to explore potential changes in high frequency variability in between different interglacial periods, Pol et al., (2010, 2011, 2014) used 11 cm resolution  $\delta D$  measurements over interglacial periods during Marine Isotopic Stages (MIS) 5, 11 and 19, i.e. the periods between 112 and 134 ka (before present), 392 and 427 ka, and 747 and 800 ka, respectively. Landais et al., (2015) focused on 11 cm resolution  $\delta^{18}O$  over the  
45 last glacial period back to 60 kyrs.

It is challenging to retrieve the absolute decadal variability from central Antarctic records (Ekaykin et al., 2017; Casado et al., 2020). But since the processes affecting the signal should not vary too much in interglacial conditions, by comparing interglacial periods MIS5 and 11 enabled to estimate the relative variations of decadal to centennial climate variability with respect to the Holocene's (Pol et al., 2011; 2014). Over the last glacial period, the high resolution  $\delta^{18}O$  record showed an  
50 enhanced amplitude of the multi-decadal to centennial variability during the warm phases of the Antarctic Isotopic Maxima, or AIM (Landais et al., 2015). These AIM events are key climatic features of the last glacial period: they are counterparts of the Northern Hemisphere abrupt temperature increases first identified in the Greenland ice cores (Dansgaard et al., 1985; Blunier and Brook, 2001; EPICA community members, 2006).

High resolution water isotopic measurements over the EDC ice core are hence key to document the temporal patterns of climatic variability over the past 800 kyrs. Unfortunately, the analytical load to obtain the full 800 kyrs record at 11 cm  
55 resolution is enormous, and would represent 35,000 measurements. Even if several individual studies have been published, a complete synthesis of EDC high resolution  $\delta D$  and  $\delta^{18}O$  records over the last 800 kyrs is still missing. This is an important limitation for the documentation of past changes in sub-orbital climatic variability in Antarctica and to compare the climatic variability features between glacial and interglacial periods or between different interglacial (glacial) periods. As an example,  
60 while we know that the interglacial periods before the Mid-Brunhes Transition (MBT, 430 ka) are cooler than the five most recent interglacial periods, we lack documentation of the high resolution climate variability during interglacial periods before and after the MBT (Barth et al., 2018; Past Interglacials Working Group of PAGES, 2016). A first challenge is thus to provide homogeneous high resolution isotopic records.

A second challenge to characterize the past high frequency climate variability in Antarctica is non-temperature related  
65 variability in the water isotopes from the depositional process (; Laepple, 2018) and smoothing / filtering effects of post-deposition processes. Indeed, post-deposition processes (Casado et al., 2020, 2018) and firn and ice diffusion (Gkinis et al.,



2011, 2021) strongly limit the interpretation of water isotopic variability in term of climatic variability. In the case of old ice, the impact of diffusion which increases with depth and age can reach multi-centennial time scales and affect the climate variability recorded in  $\delta^{18}\text{O}$  and  $\delta\text{D}$ . Pol et al. (2010) showed that the 11 cm resolution  $\delta\text{D}$  record of MIS 19 (3147 – 3190 m deep in the EDC ice core) was not bringing more information than the 55 cm resolution record because of large impact of diffusion at this depth of the core. This effect is particularly important to quantify for the 1.5 Ma ice core to be drilled in East Antarctica. Indeed, documenting the evolution of diffusion length with depth is key to anticipate what kind of information on climate variability can be retrieved from the deepest part of this future ice core.

Here we address the two aforementioned challenges (high-resolution records and influence of diffusion) by presenting a compilation of new high resolution measurements of  $\delta^{18}\text{O}$  and  $\delta\text{D}$  on the EDC ice core. The first section presents the analytical methods used to perform high resolution measurements of  $\delta\text{D}$  and  $\delta^{18}\text{O}$  of the different sections of the EDC ice core over the last decades as well as methods for spectral analyses and calculation of isotopic diffusion along the EDC ice core. The second section describes how the different measurements performed over the past 20 years in different institutes with different analytical methods can be compiled together into a single record. The third section uses the high resolution measurements to investigate changes in sub-orbital climatic variability across the last 800 kyrs and how diffusion can affect some of the observed features.

## 2. Materials and methods

### 2.1 The EPICA ice core

The Concordia Franco-Italian station is located at 3 233 m above sea level on the continental plateau of Antarctica, ( $75^{\circ}06'12''\text{S}$   $123^{\circ}21'30''\text{E}$ ). The mean annual surface temperature is  $-54.5^{\circ}\text{C}$  and the snow accumulation rate is around 25 mm water equivalent. $\text{yr}^{-1}$  (EPICA community members, 2004; Le Meur et al., 2018).

The EDC ice core has been drilled at the Concordia station on the Dome C where the ice was supposed to be the less deformed. The drilling project was conducted over the period 1996 – 2004. In 1999, the drill was stuck at 788 m depth (45 ka) so a new drilling began from the surface the same year a few meters away from the first drilling hole. The bedrock was then successfully reached in 2004 at a depth of 3190 m. This second ice core is referred as EDC2. By the time this second ice core was retrieved, the full 788 meters of EDC1 were analysed. Later, EDC2 measurements started 19 meters higher than the bottom end of the EDC1 ice core in order to have an overlap to reconnect the two cores without duplicating all the measurements on the common depth range.

After drilling and logging, the ice core was cut in 55 cm long parts. 55 cm sections were then cut longitudinally on site for several measurements (water isotopes, physical properties,  $^{10}\text{Be}$ , chemistry, gas). An archive piece (~ one quarter of the section) is stored in polystyrene boxes in the EPICA snow-cave at the Concordia station at  $-50^{\circ}\text{C}$ . Two types of samples were dedicated for the continuous analyses of water isotopes on the EDC ice core. First, a 55 cm long stick with a  $1\text{ cm}^2$  cross section was melted and stored on site in plastic bottles for the low resolution measurements. Another section (stick with  $2*1\text{ cm}$  cross



section) was cut in 5 parts of 11 cm each for the high resolution measurements and placed in plastic bags, stored at  $-20^{\circ}\text{C}$   
100 during a few months before being melted and transferred into plastic bottles kept at  $-20^{\circ}\text{C}$ .

## 2.2 Measurements techniques and coherency of the dataset

Over the last 20 years, several techniques have been applied to measure  $\delta\text{D}$  and  $\delta^{18}\text{O}$  of the EDC ice core (Tables 1 and 2).  
The first measurements on the first EDC ice core (DC-96) were performed using the uranium reduction method for  $\delta\text{D}$  (Vaughn  
et al., 1998) or the  $\text{CO}_2 - \text{H}_2\text{O}$  equilibration method for  $\delta^{18}\text{O}$  (Meyer et al., 2000). The latest measurements were performed  
105 on the EDC2 ice core using a method based on cavity ring down spectroscopy (CRDS) (Kerstel and Gianfrani, 2008; Busch  
and Busch, 1999). The precisions obtained for the different methods are comparable, i.e.  $2\sigma$  values between 1 and 1.4 ‰ for  
 $\delta\text{D}$  and between 0.1 and 0.4 ‰ for  $\delta^{18}\text{O}$  (Table 2). Figure 1 displays the full high resolution (11 cm) datasets for  $\delta^{18}\text{O}$  and  $\delta\text{D}$   
of water over the EDC ice core (figure 1).

## 2.3 The EPICA ice core

110 A discrete wavelet analysis is used to identify the contribution to the overall isotopic variability from signals of different  
periodicities (i.e. corresponding to decadal to multi-millennial signal variability). With this aim, we produced a multi resolution  
analysis (MRA) using R software with the waveslim wavelet package (Whitcher, 2020) containing the MRA function with a  
Daubechies orthonormal wavelet filter. MRA is a mathematical analysis tool which decomposes a signal at different resolution  
levels. An important feature of MRA is its ability to capture temporally localised changes at its nearest neighbour. A low  
115 (high) resolution level corresponds to a coarse (detailed/high frequency) component of the original signal. Each MRA level  
can thus be used to interpret the temporal variability within a frequency range. Adding all MRA levels exactly reproduce the  
original undecomposed signal. The wavelet analysis needs to be applied on time intervals with a uniform resolution. Because  
we aim to keep as much as possible information on the climatic variability inferred from the high resolution isotopic  
measurements, the EDC record expressed on the AICC2012 age scale has been split in 6 intervals with decreasing resolution  
120 from the top (youngest section between 0 and 56 ka where 11 cm corresponds to a 10 yr resolution on the AICC2012 age  
scale) to the bottom of the core (oldest section between 651 and 800 ka where 11 cm correspond to a 320 yr resolution on the  
AICC2012 age scale). The decomposition is explained on Table 3.

The resolution of the MRA for the different intervals was chosen to increase by a factor of two between two neighbouring  
125 intervals  $i$  and  $i+1$ ,  $i$  being a number between 1 and 5. As a consequence, the 2<sup>nd</sup> MRA decomposition of the interval  $i$  has the  
same resolution than the 1<sup>st</sup> MRA of the interval  $i+1$  (Table 3). We then concatenate the MRA with the same temporal  
resolution, leading to 9 successive composites (named a, b, c, d, e, f, g, h and i in table 3), the longest (composite f, g h and i)  
corresponding to the variability of the signal at a 320 yr resolution and covering the whole 800 kyrs and the shortest (composite  
a) corresponding to the variability of the signal at a 10 yr resolution and covering only the last 56 kyrs.



## 130 2.4 The EPICA ice core

To calculate the effect of isotopic diffusion with depth on the high resolution signal, we use the classical approach in which the initial isotopic signal is convolved with a Gaussian function  $G(z)$  of associated diffusion length  $\sigma_z$  (Gkinis, 2011; Laepple, 2018; Gkinis et al., 2021):

$$G(z) = \frac{1}{\sigma_z \sqrt{2\pi}} \exp\left(\frac{-z^2}{2\sigma_z^2}\right) \quad (1)$$

135 Where  $z$  is the depth along the ice core and  $\sigma_z$  is the diffusion length.

We quantify the amplitude decay of the signal between the initial amplitude  $A_0$  and the measured amplitude at a certain depth as described in Johnsen et al., (2000) and Gkinis et al., (2021) for given period  $\lambda$  with the following equation:

$$\frac{A}{A_0} = \exp\left(-2\left(\frac{\pi \times \sigma_z}{\lambda}\right)^2\right) \quad (2)$$

140 For our purpose, the diffusion length along the EDC ice core is calculated by considering the firn diffusion (i.e. due to water vapor diffusion in the open porosity) and the ice diffusion (i.e. due to water molecular diffusion in the ice matrix).

We used two different estimates for the firn diffusion length,  $\sigma_{\text{firn}}$ , along the EDC ice core. In a first approach, we assumed a constant  $\sigma_{\text{firn}}$  all along the EDC ice core and take the value of 0.07 m estimated by Johnsen et al. (2000) for EDC. In a second refined approach, we considered a changing  $\sigma_{\text{firn}}$  between interglacial and glacial periods as described in (Gkinis et al., 2021).

145 This leads to a  $\sigma_{\text{firn}}$  varying between 0.075 m in interglacial period to 0.065 m in glacial period. The ice thinning,  $S$ , also affects the visible effect of firn diffusion length along the ice core so that the thinned firn diffusion length should be  $\sigma_{\text{thinned\_firn}} = S \times \sigma_{\text{firn}}$ . In this study, for consistency, we used the thinning function for the EDC ice core corresponding to the AICC2012 chronology (Bazin et al., 2013).

The ice diffusion depends on the thinning and the temperature. The following formulation permits to calculate the diffusion length associated with ice diffusion,  $\sigma_{\text{ice}}$ , as a function of age (and also depth) of the ice (Gkinis et al., 2011) :

$$\sigma_{\text{ice}}^2(\tau) = S(\tau)^2 \int_0^\tau 2D(t)S(t)^{-2} dt \quad (3)$$

With  $S$  the thinning of the ice layers at the considered age  $\tau$ . In order to estimate the ice diffusion coefficient  $D(t)$ , we use the classical formulation of Ramseier (1967):

$$D = D_0 \times \exp\left(\frac{-Q}{RT}\right) \quad (4)$$

155 with  $D_0 = 9.13 \text{ cm}^2/\text{s}$  and  $Q = 59.820 \text{ kJ/mol}$ . At  $-50^\circ\text{C}$ ,  $D$  is equal  $8.866 \cdot 10^{-14} \text{ cm}^2/\text{s}$  and at  $-10^\circ\text{C}$ ,  $D$  is equal to  $1.1993 \cdot 10^{-11} \text{ cm}^2/\text{s}$ ,  $T$  represents the ice temperature from the borehole.

The total calculated diffusion length expected to be measured in the ice core could then be estimated using the diffusion length associated with the firn diffusion and the diffusion length associated with ice diffusion in a quadratic addition, so that:



$$\sigma_z = \sqrt{(\sigma_{\text{ice}}^2 + \sigma_{\text{thinned\_firn}}^2)} \quad (5)$$

160 The increase of the diffusion length for increasing depth in the ice core is shown in Figure S1. It is mainly due to the increase in temperature. The borehole temperature indeed evolves almost linearly from  $-53.5^{\circ}\text{C}$  to  $-2.6^{\circ}\text{C}$  along the 3255 m ice core (Buizert et al., 2021). The variation of the calculated diffusion length around 3000 m is explained by the variability of the thinning function (Dreyfus et al., 2007).

### 165 3. The EPICA ice core

Because  $\delta^{18}\text{O}$  and  $\delta\text{D}$  measurements were performed over a long period in different institutes using different methods, we checked the coherency of the different datasets in two different ways: 1/ comparison of the same samples measured by different techniques on different periods and 2/ comparison of the low resolution measurements (55 cm resolution) with a 5 points average of the high resolution measurements (11 cm resolution).

170 First, we used the new CRDS technique in 2019-2020 to measure two sets of samples already analysed within the period 2004-2010 by uranium reduction for  $\delta\text{D}$  on MIS 5.5 (1670-1693 m) and by  $\text{H}_2\text{O}-\text{CO}_2$  equilibration for  $\delta^{18}\text{O}$  (1670-1793 m). Figures 2 and 3 provide two examples of analyses performed on all overlapping intervals. Additional comparisons of new vs old data are also presented in the supplementary material sections (Figure S5 and S6). The difference between the old and the new  $\delta\text{D}$  series (Figure 2) seems to depend on the absolute value for  $\delta\text{D}$  (negative difference for low  $\delta\text{D}$  values). This is confirmed  
175 through a statistical test on the correlation between the absolute value of  $\delta\text{D}$  and the  $\delta\text{D}$  difference between the two series of measurements leading to a Pearson coefficient of 0.13 and a p-value of 0.003. Such an isotopic-dependent feature may arise from a possible calibration effect despite the fact that exchanges of home water standards and regular intercalibrations were performed between the laboratories measuring water isotopes of the EDC ice cores.

Despite such tendency in the  $\delta\text{D}$  differences between the two series, the absolute value of the difference remains small. We  
180 use a Welch t-test to show that the old and new time series have equal means at a 99.9 % confidence level ( $t=3.5$ ,  $N=1000$ ) with respect to the experimental margin of errors.

Finally, the distribution of the differences between the first and the new  $\delta\text{D}$  measurements is not Gaussian and not centred around 0. Still, this distribution is narrower ( $2\sigma = 0.8 \text{ ‰}$  when fitted by a Gaussian curve) than a Gaussian distribution with  $2\sigma = 1.4 \text{ ‰}$  associated with the classical analytical uncertainty of the  $\delta\text{D}$  measurements. The analytical uncertainty associated  
185 with the CRDS measurements series has been evaluated from the analysis of the difference between the same samples (1000 samples, which represent 10 % of the whole series) measured twice, 1 to 3 months apart. The distribution of the difference between duplicated analyses of the same samples with the same method is Gaussian with 33 % of the  $\delta\text{D}$  difference being higher than 0.7 ‰. We conclude that both  $\delta\text{D}$  series are comparable.

In parallel, no dependence on  $\delta^{18}\text{O}$  values is observed for the distribution of the differences between the old and new  $\delta^{18}\text{O}$   
190 series. The standard deviation of the series of difference between old and new  $\delta^{18}\text{O}$  measurements ( $2\sigma = 0.2 \text{ ‰}$ ) is smaller



than the classical analytical uncertainty of the  $\delta^{18}\text{O}$  measurements by CRDS ( $2\sigma = 0.4 \text{ ‰}$ ) (Figure 3). A statistical test was made on the correlation between the absolute value of  $\delta^{18}\text{O}$  and the  $\delta^{18}\text{O}$  difference between the two series of measurements leading to a Pearson coefficient of 0.0049 and a p-value of 0.9. In addition, we did a Welch t-test of the equality between two averages in  $\delta^{18}\text{O}$  to know if the difference between the old and new  $\delta^{18}\text{O}$  data is significantly different within the experimental margin of error. When doing so, the result shows that the two series have equal means at a 70 % confidence level ( $t=0.557$ ,  $N=1000$ ).

Second, we compared low (55 cm) and high resolution (11 cm)  $\delta^{18}\text{O}$  series after gathering the five 11 cm neighbour samples (Figures S2 to S4). The difference between the two timeseries is  $0.008 \pm 0.001 \text{ ‰}$  (Figure S4). The comparison between low and high resolution series for  $\delta\text{D}$  was already performed by (Pol et al., 2011, 2014). In the 2011 paper, the coherency between 55 cm and 11 cm samples was studied through the calculation of the average signal over five 11 cm data. They observed that the signal from the 55 cm samples is similar to the average signal with however a lower statistical accuracy ( $1\sigma = 0.5 \text{ ‰}$ ) than the average signal ( $1\sigma = 0.23 \text{ ‰}$ ).

The two comparisons performed above lead to the conclusion that the different  $\delta^{18}\text{O}$  and  $\delta\text{D}$  EDC datasets gathered here and displayed on Figure 1 are coherent. It is thus reasonable to merge all the datasets together and create a unique high resolution time serie containing all data obtained within different laboratories at different periods and with different techniques.

## 4. Results and discussion

### 4.1 Recorded multi-decadal to multi-millennial isotopic variability over the last 800 kyrs

The compiled high resolution water isotope datasets on the EDC ice core is presented in Figure 1. For  $\delta\text{D}$ , 5 interglacial periods have been analyzed at high resolution. For  $\delta^{18}\text{O}$ , we have a profile almost complete except MIS 7 and part of MIS 11. We use these times series to study the multi-decadal to millennial variability over the last 800 kyrs, extending the results of Pol et al., (2011, 2014), which focused on the evolution of the multi-decadal and multi-centennial variability during the Holocene, MIS 5 and MIS 11.

We applied the MRA decomposition on each of the 6 selected intervals (see Methods) and present decadal to multi-millennial variability across the last 800 000 years (Fig. 4). We calculated the running standard deviation ( $1\sigma$ ) on a 3 ka window and we use this value as an estimate of the level of variability. For the first MRA composite at 10yr resolution (a), we observe a stronger isotopic variability during the Holocene than during the Last Glacial Maximum (average  $1\sigma$  of 0.46 ‰ and 0.24 ‰, respectively). The 20 yr variability (b) inferred from the second composite shows a globally uniform pattern over the last 150 kyrs. The 80 yr variability (d) is smaller during the interglacial periods ( $1\sigma=0.18 \text{ ‰}$ ) than during the glacial periods ( $1\sigma=0.30 \text{ ‰}$ ) over the last 400 kyrs. The 160 to 640 yr variability (e to g) also shows a small decrease of variability over interglacial periods and decreasing variability for the oldest ice core sections. For the lower frequency variabilities (composite at 1280 and 2560 yr resolution, h to i) the amplitude of the variability envelope increases during glacial inception and glacial period with





225 a notable strong 2560 yr variability at the onset of MIS 9 ( $1\sigma=1.13\text{ ‰}$  compared to an average of  $1\sigma=0.20\text{ ‰}$  over the whole series). The large centennial to multi-centennial water isotope variability in glacial periods can be linked to the succession of the Antarctic Isotopic Maxima (AIM) during glacial periods (EPICA community members, 2004; Jouzel et al., 2007). Finally, the decreasing amplitude of the signal variability toward old ages is probably the result of diffusion of water isotopes in firn open porosity and ice crystal. While we can disentangle the effect of diffusion and climate driven isotopic variability for low frequency signal and deep depth, the respective influences of diffusion and climate are less obvious to identify at shallower depths and for high frequencies.

#### 230 **4.2 Effect of isotopic diffusion on the recorded signal variability**

We evaluate the effects of diffusion on the isotopic signal recorded in ice core records by computing the decrease of Holocene variability from equation (2). The calculated  $A/A_0$  signal amplitude is hence scaled for each MRA composites to the mean amplitude of the variability of the MRA composite signal between 2 and 8 ka for each resolution (Figure 6).

235 As explained in the section “methods”, we used the ice diffusion coefficient from Ramseier (1967) with 2 different estimates for  $\sigma_{\text{firn}}$ . The different estimates of  $\sigma_{\text{firn}}$  do not have a significant effect on the calculated amplitude of the variability (Figure 5).

240 Diffusion has the expected effect to decrease the amplitude of the variability of the isotopic signal for older and deeper ice core sections. On the 10 yr series (a), diffusion dampens by half the amplitude of the recorded variability of the last glacial period compared to the Holocene. The calculated amplitude of the variability due to diffusion is actually much smaller than the recorded one which suggests that either the 10 yr isotopic variability during the last glacial period is larger than the 10 yr variability during the Holocene or that measurement noise is dominating the 10 yr variability.

For the bottom part of the ice core, i.e. sections older than 600 kyrs, the diffusion model overestimates the damping of centennial and multi-centennial variability compared to what is retrieved from the ice core isotopic composition. This discrepancy calls for future reassessment of the isotopic diffusivity in the bottom part of the EDC ice core.

245

#### **4.2 The climatic variability at different timescales over the last 800 kyrs**

Combining our high resolution water isotopic records with frequency analysis and the impact of diffusion, we can suggest some patterns for the decadal to millennial climate variability over the last 800 kyrs.

250 First, at the decadal scale, our findings can be interpreted as a larger variability during the last glacial period compared to the Holocene. The analysis of (Jones et al., 2017) using water isotopic record on the WAIS Divide record in West Antarctica supports this higher variability at the decadal scale during the last glacial maximum. In this high accumulation site, diffusion is not affecting much the variability with a 4-15 yr periodicity and the higher water isotopic variability observed during this period is interpreted as an increase in the strength of the teleconnections between the tropical Pacific and West Antarctica. This increase should be related to the increase of the Northern Hemisphere leading to a shift in the location of the tropical





255 convection. The same pattern is observed for the 20 yr periodicity (Figure 5, panel b), i.e. the calculated diffused variability is smaller than the measured one during the last glacial period while there is a good agreement between diffused and measured signal over MIS 5e. For the 40 and 320 yr periodicity (Figure 5, c to f), the variability of the last glacial period is also higher than the diffused Holocene variability. It is also the case for MIS 6 for the 80 yr periodicity (Figure 5, d) and MIS 8 and 10 for the 160 and 320 yr periodicity (Figure 5 e to f). For these periods and frequency ranges, the impact of diffusion on the variability is limited, and the isotopic signal in the ice core preserved. The multi-centennial variability increase during glacial periods can be related to the presence of AIM.

Our analysis hence shows that there is a clear enhanced isotopic variability during glacial periods at the multi-decadal to multi-centennial timescale in the EDC ice core which could be attributed to climate variability. This result is in agreement with the findings of Rehfeld et al. (2018) using a worldwide data synthesis showing increased interannual to millennial climatic variability during the last glacial maximum with respect to the Holocene at all latitudes with an increase of the variance by a factor of 2 in the high latitudes of the Southern Hemisphere, a result in agreement with output of coupled model simulations (Rehfeld et al., 2018).

Second, while the effect of diffusion is important when we want to compare variability from one interglacial periods to another, it does not affect much the evolution of the recorded variability during the course of an interglacial period.

270 In their previous study focused on the warm phase of MIS 5 (115.5 to 132 ka), Pol et al. (2014) used wavelet analysis of the 11cm resolution  $\delta D$  record and evidenced three different phases with different level of variability. The first phase from 111 to 119 ka has a low orbital forcing context but the variability increases during the entry in glaciation, with centennial dominant periodicities. The second phase from 119 to 123 ka is a stable warm phase, warmer than the Holocene. The  $\delta D$  variability of the second phase is notably lower than the other phases, 3.7 ‰ compared to a 4.5 ‰ average. Finally, during the third phase there is again a higher variability with dominant multi centennial periodicities between 123 and 133 ka.

When doing a similar analysis with our MRA decomposition, we find similar variability of the high resolution signal (Figure 6 a), i.e. the maximum amplitude of the multi-decadal to multi-centennial variability of the signal is encountered over the optimum of MIS 5 (phase 3 in Pol et al., (2014), between 125 and 131 ka) and toward end of this warm period (phase 1 of Pol et al., (2014)). The minimum amplitude of the multi-decadal to multi-centennial variability of the signal is encountered between 119 and 123 ka (phase 2 in Pol et al., (2014)) when the  $\delta^{18}O$  and  $\delta D$  signals are on a plateau.

280 Thus, during MIS 5, multi-decadal to multi-centennial variability of the water isotopic signal can be interpreted as climate variability at these multi-decadal to multi-centennial timescales. It can be compared to the variability over the interglacial period of MIS 9 (~ between 325 and 338.5 ka) also characterized by a temperature optimum at its start. The amplitudes of the variability for the different MRA decompositions for the interglacial period of MIS 9 cannot be directly compared to ones over MIS 5 because of the effect of diffusion and thinning (see figure 5). However, in figure 6 b we observe the same pattern than for MIS5: higher amplitudes for the multi-decadal to multi-centennial variability are observed over the  $\delta^{18}O$  optimum (333 – 338 ka) and at the end of this warm period (321 – 326 ka) while the minimum amplitudes for the multi-decadal to multi-centennial variability is observed over the plateau of the interglacial period (326 – 332 ka). This result strengthens the



290 conclusion of Pol et al. (2014) that the climate over temperature optimum of interglacial periods may also be more variable at  
the multi-decadal to multi-centennial timescale. A parallel can be drawn with the higher high frequency water isotopic  
variability observed during temperature optimum of the AIM of the last glacial period on the EDC ice core (Landais et al.,  
2015) since this temperature optimum at the beginning of the interglacial could also be the result of millennial scale variability  
(Past Interglacials Working Group of PAGES, 2016).

## 5 Conclusion

295 We presented a synthesis of new and published 11 cm resolution profiles of  $\delta D$  and  $\delta^{18}O$  over the last 800 kyrs on the EDC  
ice core. We showed that the various water isotopic data measured by different laboratories and techniques over the last 20  
years have coherent calibrations and homogeneous quality within analytical uncertainty. As a result, they can be combined  
and we provide here a homogenous and complete data series of high resolution water isotopes of the EDC ice core.

300 A MRA decomposition of the water isotopic record at temporal resolution varying between 10 and 2560 years shows that the  
variability during glacial periods at multi decadal to multi centennial timescale is higher than variability of the Holocene and  
that the variability is enhanced over early temperature optimum during MIS 5 and 9. These results are not influenced by  
diffusion in the firn open porosity and in the ice matrix but the interpretation of high resolution  $\delta D$  and  $\delta^{18}O$  profiles should  
take this effect into account. Finally, our study calls for further analyses for quantifying the diffusivity in EDC which is  
essential in the perspective of the BE-OI ice core.

305



## References

- Barth, A. M., Clark, P. U., Bill, N. S., He, F., and Piasias, N. G.: Climate evolution across the Mid-Brunhes Transition, *Clim. Past*, 14, 2071–2087, <https://doi.org/10.5194/cp-14-2071-2018>, 2018.
- 310 Bazin, L., Landais, A., Lemieux-Dudon, B., Toyé Mahamadou Kele, H., Veres, D., Parrenin, F., Martinerie, P., Ritz, C., Capron, E., Lipenkov, V., Loutre, M.-F., Raynaud, D., Vinther, B., Svensson, A., Rasmussen, S. O., Severi, M., Blunier, T., Leuenberger, M., Fischer, H., Masson-Delmotte, V., Chappellaz, J., and Wolff, E.: An optimized multi-proxy, multi-site Antarctic ice and gas orbital chronology (AICC2012): 120–800 ka, *Clim. Past*, 9, 1715–1731, <https://doi.org/10.5194/cp-9-1715-2013>, 2013.
- 315 Bereiter, B., Eggleston, S., Schmitt, J., Nehrbass-Ahles, C., Stocker, T. F., Fischer, H., Kipfstuhl, S., and Chappellaz, J.: Revision of the EPICA Dome C CO<sub>2</sub> record from 800 to 600 kyr before present: Analytical bias in the EDC CO<sub>2</sub> record, *Geophys. Res. Lett.*, 42, 542–549, <https://doi.org/10.1002/2014GL061957>, 2015.
- Blunier, T. and Brook, E. J.: Timing of Millennial-Scale Climate Change in Antarctica and Greenland During the Last Glacial Period, *Science*, 291, 109–112, <https://doi.org/10.1126/science.291.5501.109>, 2001.
- 320 Buizert C., Fudge T. J., Roberts W. H. G., Steig E. J., Sherriff-Tadano S., Ritz C., Lefebvre E., Edwards J., Kawamura K., Oyabu I., Motoyama H., Kahle E. C., Jones T. R., Abe-Ouchi A., Obase T., Martin C., Corr H., Severinghaus J. P., Beaudette R., Epifanio J. A., Brook E. J., Martin K., Chappellaz J., Aoki S., Nakazawa T., Sowers T. A., Alley R. B., Ahn J., Sigl M., Severi M., Dunbar N. W., Svensson A., Fegyveresi J. M., He C., Liu Z., Zhu J., Otto-Bliesner B. L., Lipenkov V. Y., Kageyama M., and Schwander J.: Antarctic surface temperature and elevation during the Last Glacial Maximum, *Science*, 372, 1097–1101, <https://doi.org/10.1126/science.abd2897>, 2021.
- 325 Busch, K. W. and Busch, M. A. (Eds.): *Cavity-Ringdown Spectroscopy: An Ultratrace-Absorption Measurement Technique*, American Chemical Society, Washington, DC, <https://doi.org/10.1021/bk-1999-0720>, 1999.
- Casado, M., Landais, A., Picard, G., Münch, T., Laepple, T., Stenni, B., Dreossi, G., Ekaykin, A., Arnaud, L., Genthon, C., Touzeau, A., Masson-Delmotte, V., and Jouzel, J.: Archival processes of the water stable isotope signal in East Antarctic ice cores, *The Cryosphere*, 12, 1745–1766, <https://doi.org/10.5194/tc-12-1745-2018>, 2018.
- 330 Casado, M., Münch, T., and Laepple, T.: Climatic information archived in ice cores: impact of intermittency and diffusion on the recorded isotopic signal in Antarctica, *Clim. Past*, 16, 1581–1598, <https://doi.org/10.5194/cp-16-1581-2020>, 2020.
- Dansgaard, W.: Greenland ice core studies. *Paleogeography, Paleoclimatology, Paleoecology*, 50: 185-187, 1985.
- 335 Dreyfus, Parrenin, F., Barnola, J.-M., Beer, J., Blunier, T., Castellano, E.: The EDC3 chronology for the EPICA Dome C ice core. *Climate of the Past Discussions*, pp.575-606, 2007.
- Ekaykin, A. A., Lipenkov, V. Ya., Barkov, N. I., Petit, J. R., and Masson-Delmotte, V.: Spatial and temporal variability in isotope composition of recent snow in the vicinity of Vostok station, Antarctica: implications for ice-core record interpretation, *Ann. Glaciol.*, 35, 181–186, <https://doi.org/10.3189/172756402781816726>, 2002.
- 340 EPICA community members: Eight glacial cycles from an Antarctic ice core, *Nature*, 429, 623–628, <https://doi.org/10.1038/nature02599>, 2004.
- Fisher D. A., Reeh, N., Clausen, H.B.: Stratigraphic noise in time series derived from ice cores. *Annals of glaciology* 7, 1985.
- Gkinis, V., Ph.D. thesis, University of Copenhagen, Center for Ice and Climate (2011): High resolution water isotope data from ice cores.



- 345 Gkinis, V., Popp, T. J., Blunier, T., Bigler, M., Schüpbach, S., and Johnsen, S. J.: Water isotopic ratios from a continuously melted ice core sample, Others (Wind, Precipitation, Temperature, etc.)/Laboratory Measurement/Instruments and Platforms, <https://doi.org/10.5194/amtd-4-4073-2011>, 2011.
- Gkinis, V., Holme, C., Kahle, E. C., Stevens, M. C., Steig, E. J., and Vinther, B. M.: Numerical experiments on firn isotope diffusion with the Community Firn Model, *J. Glaciol.*, 67, 450–472, <https://doi.org/10.1017/jog.2021.1>, 2021.
- 350 Gkinis, V.; Dahl-Jensen, D.; Steffensen, J. P.; Vinther, B. M.; Landais, A.; Jouzel, J.; Masson-Delmotte, V.; Cattani, O.; Minster, B.; Grisart, A.; Hörhold, M.; Stenni, B.; Selmo, E. (2021b): Oxygen-18 isotope ratios from the EPICA Dome C ice core at 11 cm resolution. PANGAEA, <https://doi.org/10.1594/PANGAEA.939445>
- 355 Helsen, M. M., van de Wal, R. S. W., van den Broeke, M. R., Masson-Delmotte, V., Meijer, H. A. J., Scheele, M. P., and Werner, M.: Modeling the isotopic composition of Antarctic snow using backward trajectories: Simulation of snow pit records, *J. Geophys. Res.*, 111, D15109, <https://doi.org/10.1029/2005JD006524>, 2006.
- Johnsen, Cuffey, K. M., Schwander, J., and Creyts, T.: Diffusion of stable isotopes in polar firn and ice : the isotope effect in firn diffusion, 21, 2000.
- 360 Jones, T. R., Cuffey, K. M., White, J. W. C., Steig, E. J., Buizert, C., Markle, B. R., McConnell, J. R., and Sigl, M.: Water isotope diffusion in the WAIS Divide ice core during the Holocene and last glacial, *J. Geophys. Res. Earth Surf.*, 122, 290–309, <https://doi.org/10.1002/2016JF003938>, 2017.
- Jouzel, J., Masson-Delmotte, V., Cattani, O., Dreyfus, G., Falourd, S., Hoffmann, G., Minster, B., Nouet, J., Barnola, J. M., Chappellaz, J., Fischer, H., Gallet, J. C., Johnsen, S., Leuenberger, M., Loulergue, L., Luethi, D., Oerter, H., Parrenin, F., 365 Raisbeck, G., Raynaud, D., Schilt, A., Schwander, J., Selmo, E., Souchez, R., Spahni, R., Stauffer, B., Steffensen, J. P., Stenni, B., Stocker, T. F., Tison, J. L., Werner, M., and Wolff, E. W.: Orbital and Millennial Antarctic Climate Variability over the Past 800,000 Years, *Science*, 317, 793–796, <https://doi.org/10.1126/science.1141038>, 2007.
- Jouzel, J., Delaygue, G., Landais, A., Masson-Delmotte, V., Risi, C., and Vimeux, F.: Water isotopes as tools to document oceanic sources of precipitation: Water Isotopes and Precipitation Origin, *Water Resour. Res.*, 49, 7469–7486, 370 <https://doi.org/10.1002/2013WR013508>, 2013.
- Kerstel, E. and Gianfrani, L.: Advances in laser-based isotope ratio measurements: selected applications, *Appl. Phys. B*, 92, 439–449, <https://doi.org/10.1007/s00340-008-3128-x>, 2008.
- Laepple, T., Münch, T., Casado, M., Hoerhold, M., Landais, A. and Kipstuhl, S.: On the similarity and apparent cycles of isotopic variations in East Antarctic snow pits, *Cryosphere* 12(1), 169–187, doi:10.5194/tc-12-169-2018, 2018.
- 375 Landais, A., Masson-Delmotte, V., Stenni, B., Selmo, E., Roche, D. M., Jouzel, J., Lambert, F., Guillevic, M., Bazin, L., Arzel, O., Vinther, B., Gkinis, V., and Popp, T.: A review of the bipolar see–saw from synchronized and high resolution ice core water stable isotope records from Greenland and East Antarctica, *Quat. Sci. Rev.*, 114, 18–32, <https://doi.org/10.1016/j.quascirev.2015.01.031>, 2015.
- 380 Landais, A., Stenni, B., Masson-Delmotte, V., Jouzel, J., Cauquoin, A., Fourré, E., Minster, B., Selmo, E., Extier, T., Werner, M., Vimeux, F., Uemura, R., Crotti, I., and Grisart, A.: Interglacial Antarctic–Southern Ocean climate decoupling due to moisture source area shifts, *Nat. Geosci.*, 14, 918–923, <https://doi.org/10.1038/s41561-021-00856-4>, 2021.
- Laskar, J., Robutel, P., Joutel, F., Gastineau, M., Correia, A. C. M., and Levrard, B.: A long-term numerical solution for the insolation quantities of the Earth, *Astron. Astrophys.*, 428, 261–285, <https://doi.org/10.1051/0004-6361:20041335>, 2004.



- 385 Le Meur, E., Magand, O., Arnaud, L., Fily, M., Frezzotti, M., Cavitte, M., Mulvaney, R., and Urbini, S.: Spatial and temporal distributions of surface mass balance between Concordia and Vostok stations, Antarctica, from combined radar and ice core data: first results and detailed error analysis, *The Cryosphere*, 12, 1831–1850, <https://doi.org/10.5194/tc-12-1831-2018>, 2018.
- 390 Lüthi, D., Le Floch, M., Bereiter, B., Blunier, T., Barnola, J.-M., Siegenthaler, U., Raynaud, D., Jouzel, J., Fischer, H., Kawamura, K., and Stocker, T. F.: High-resolution carbon dioxide concentration record 650,000–800,000 years before present, *Nature*, 453, 379–382, <https://doi.org/10.1038/nature06949>, 2008.
- Meyer, H., Schöncke, L., Wand, U., Hubberten, H. W., and Friedrichsen, H.: Isotope Studies of Hydrogen and Oxygen in Ground Ice - Experiences with the Equilibration Technique, *Isotopes Environ. Health Stud.*, 36, 133–149, <https://doi.org/10.1080/10256010008032939>, 2000.
- 395 Noone, D.: Sea ice control of water isotope transport to Antarctica and implications for ice core interpretation, *J. Geophys. Res.*, 109, D07105, <https://doi.org/10.1029/2003JD004228>, 2004.
- Past Interglacials Working Group of PAGES: Interglacials of the last 800,000 years, *Rev. Geophys.*, 54, 162–219, <https://doi.org/10.1002/2015RG000482>, 2016.
- 400 Pol, K., Masson-Delmotte, V., Johnsen, S., Bigler, M., Cattani, O., Durand, G., Falourd, S., Jouzel, J., Minster, B., and Parrenin, F.: New MIS 19 EPICA Dome C high resolution deuterium data: Hints for a problematic preservation of climate variability at sub-millennial scale in the “oldest ice,” *Earth Planet. Sci. Lett.*, 298, 95–103, <https://doi.org/10.1016/j.epsl.2010.07.030>, 2010.
- 405 Pol, K., Debret, M., Masson-Delmotte, V., Capron, E., Cattani, O., Dreyfus, G., Falourd, S., Johnsen, S., Jouzel, J., Landais, A., Minster, B., and Stenni, B.: Links between MIS 11 millennial to sub-millennial climate variability and long term trends as revealed by new high resolution EPICA Dome C deuterium data – A comparison with the Holocene, *Clim. Past*, 7, 437–450, <https://doi.org/10.5194/cp-7-437-2011>, 2011.
- Pol, K., Masson-Delmotte, V., Cattani, O., Debret, M., Falourd, S., Jouzel, J., Landais, A., Minster, B., Mudelsee, M., Schulz, M., and Stenni, B.: Climate variability features of the last interglacial in the East Antarctic EPICA Dome C ice core, *Geophys. Res. Lett.*, 41, 4004–4012, <https://doi.org/10.1002/2014GL059561>, 2014.
- 410 Ramseier, R. O.: Self-diffusion of tritium in natural and synthetic ice monocrystals, *Journal of applied physics* 38, 2553 1967. doi: 10.1063/1.1709948
- Rehfeld, K., Münch, T., Ho, S. L., and Laepple, T.: Global patterns of declining temperature variability from the Last Glacial Maximum to the Holocene, *Nature*, 554, 356–359, <https://doi.org/10.1038/nature25454>, 2018.
- 415 Stenni, B., Jouzel, J., Masson-Delmotte, V., Röthlisberger, R., Castellano, E., Cattani, O., Falourd, S., Johnsen, S. J., Longinelli, A., and Sachs, J. P.: A late-glacial high-resolution site and source temperature record derived from the EPICA Dome C isotope records (East Antarctica), *Earth Planet. Sci. Lett.*, 217, 183–195, [https://doi.org/10.1016/S0012-821X\(03\)00574-0](https://doi.org/10.1016/S0012-821X(03)00574-0), 2004.
- 420 Stenni, B., Masson-Delmotte, V., Selmo, E., Oerter, H., Meyer, H., Röthlisberger, R., Jouzel, J., Cattani, O., Falourd, S., Fischer, H., Hoffmann, G., Iacumin, P., Johnsen, S. J., Minster, B., and Udisti, R.: The deuterium excess records of EPICA Dome C and Dronning Maud Land ice cores (East Antarctica), *Quat. Sci. Rev.*, 29, 146–159, <https://doi.org/10.1016/j.quascirev.2009.10.009>, 2010.



Vaughn, B. H., White, J. W. C., Delmotte, M., Trolier, M., Cattani, O., and Stievenard, M.: An automated system for hydrogen isotope analysis of water, *Chem. Geol.*, 152, 309–319, [https://doi.org/10.1016/S0009-2541\(98\)00117-X](https://doi.org/10.1016/S0009-2541(98)00117-X), 1998.

425 Veres, D., Bazin, L., Landais, A., Toyé Mahamadou Kele, H., Lemieux-Dudon, B., Parrenin, F., Martinerie, P., Blayo, E., Blunier, T., Capron, E., Chappellaz, J., Rasmussen, S. O., Severi, M., Svensson, A., Vinther, B., and Wolff, E. W.: The Antarctic ice core chronology (AICC2012): an optimized multi-parameter and multi-site dating approach for the last 120 thousand years, *Clim. Past*, 9, 1733–1748, <https://doi.org/10.5194/cp-9-1733-2013>, 2013.

Whitcher, B., 2020: Package Waveslim, Basic wavelet routines for one-, two-, and three dimensional signal processing, version 1.8.2, License BSD\_3\_clause, CRAN.

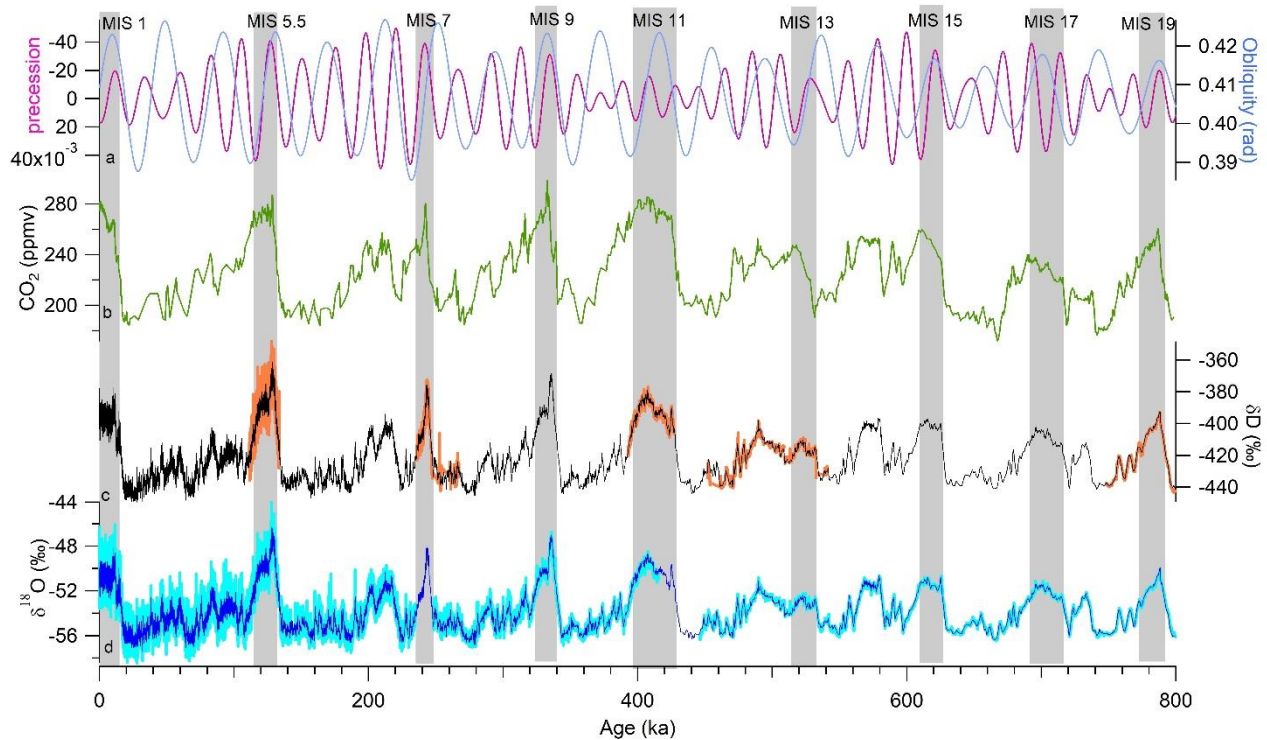
#### 430 **Acknowledgement**

This work is a contribution to the European Project for Ice Coring in Antarctica (EPICA), a joint European Science Foundation and European Commission scientific program, funded by the European Union and by national contributions from Belgium, Denmark, France, Germany, Italy, Netherlands, Norway, Sweden, Switzerland, and the United Kingdom. The main logistic support was provided by Institut Polaire Français Paul-Emile Victor and Programma Nazionale Ricerche in Antartide.

435 A.G. was supported by the European Research Council under the European Union Horizon 2020 Programme ERC ICORDA (817493).



## Figures



440 **Figure 1: High resolution water isotopic records over the last 800 kyrs on the EDC ice core. (a) precession (pink) and obliquity (blue)** from Laskar et al., (2004); **(b) Composite EDC and Vostok CO<sub>2</sub> record over the last 800 kyrs (Lüthi et al., 2008; Bereiter et al., 2015); (c) 11 cm (orange) and 55 cm resolution (black) of the EDC  $\delta D$  record; (d) 11 cm (light blue) and 55 cm resolution (dark blue) of the EDC  $\delta^{18}O$  record. All ice core records are presented on the AICC2012 scale (Bazin et al., 2013; Veres et al., 2013). Grey rectangles indicate the position of interglacial periods.**

445





Place of measurements	Date	Age (ka)	Depth (m)	Resolution (m)	Method	2 $\sigma$ (‰)	Reference
LSCE	2010	112-134	1489-1756	0.11	Uranium reduction	1	(Pol et al., 2014)
	2002 - 2007	0-27 0-800	0-577 0-3189	0.55			(Jouzel et al., 2001) (Jouzel et al., 2007)
	2021	235-245	2253-2308	0.11		1	This study
	2011	392-427	2694-2779	0.11		1	(Pol et al., 2011)
	2010	747-801	3146-3189	0.11		1	(Pol et al., 2010)
	2019	127-128.5 129.2-133 133.8-138	1670-1693 1704-1748 1756-1782	0.11	CRDS spectroscopy analyser	1.4	This study
	2019	245-267	2309-2372	0.11		1.4	This study
	2019	451-542	2799-2913	0.11		1.4	This study
	2019 - 2020	450-802	2772-3035 3044-3190	0.55		1.4	(Landais et al., 2021)

**Table 1: Summary of available  $\delta D$  measurements on the EDC ice core and associated analytical methods.  $2\sigma$  values come from instrumental measurement uncertainty as provided in the original studies.**



Place of measurements	Date	Age (ka)	Depth (m)	Resolution (m)	Method	2σ (‰)	Reference	
LSCE	2019	127-128.5	1670-1693	0.11	CRDS spectroscopy analyser	0.4	This study	
		129.2-133	1704-1748					
		133.8-138	1756-1782					
	2019	245-267	2309-2372	0.11		0.4	This study	
2019	451-542	2799-2913	0.11	0.4	This study			
2019-2020	450-802	2772-3035 3044-3190	0.55	0.4	(Landais et al., 2021)			
University of Copenhagen	2001-2010	0-3	6.6-120	0.11	CO <sub>2</sub> equilibration	0.14	(Gkinis 2011) (Landais et al., 2015) (Gkinis et al. 2021 b)	
		3-3.6	120-134					
		7-9	234-288					
		9.3-34.2	290-656					
		34.5-60	659-946					
		60-115	946-1528					
		2021	116-120					1539-1583
		121-124	1594-1638					
	125-128	1649-1693						
	129-133	1704-1748						
	134-142	1759-1803						
	248-415	2317-2756						
543-802	2794-3190							
University of Trieste	2001	0-27	0-590	0.55		0.2	(Stenni et al., 2001)	
University of Parma	2004	0-44.8	0-787				(Stenni et al., 2004)	
University of Parma	2010	0-140	0-1790				(Stenni et al., 2010)	
University of Parma	2021	0-800	0-3190				(Landais et al., 2021)	

**Table 2: Summary of available δ<sup>18</sup>O measurements on the EDC ice core and associated analytical methods. 2σ values come from instrumental measurement uncertainty as provided in the original studies.**

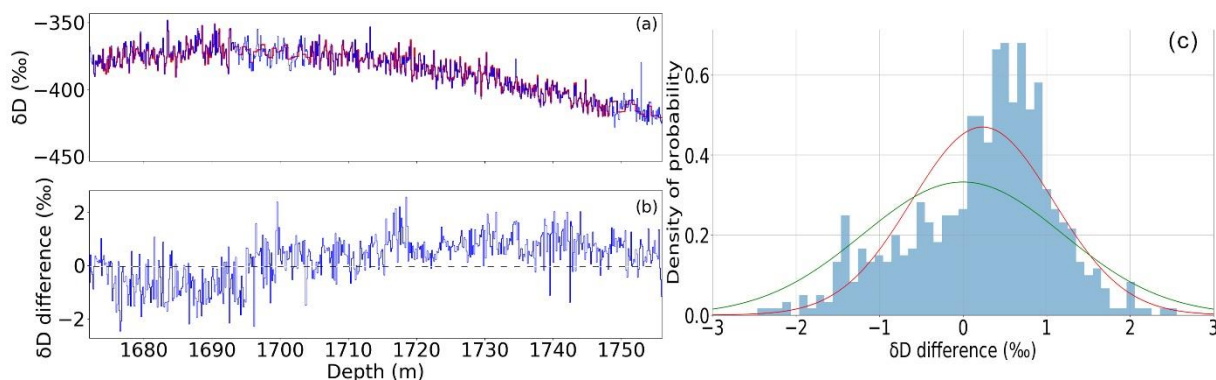


455

Interval Decom Positions	Interval 1 (0-56 kyrs)	Interval 2 (56 - 144 kyrs)	Interval 3 (144 - 305 kyrs)	Interval 4 (305 - 420 kyrs)	Interval 5 (420 - 651 kyrs)	Interval 6 (651 - 800 kyrs)
MRA 1	10 (a)	20 (b)	40 (c)	80 (d)	160 (e)	320 (f)
MRA 2	20 (b)	40 (c)	80 (d)	160 (e)	320 (f)	640 (g)
MRA 3	40 (c)	80 (d)	160 (e)	320 (f)	640 (g)	1280 (h)
MRA 4	80 (d)	160 (e)	320 (f)	640 (g)	1280 (h)	2560 (i)
MRA 5	160 (e)	320 (f)	640 (g)	1280 (h)	2560 (i)	
MRA 6	320 (f)	640 (g)	1280 (h)	2560 (i)		
MRA 7	640 (g)	1280 (h)	2560 (i)			
MRA 8	1280 (h)	2560 (i)				
MRA 9	2560 (i)					

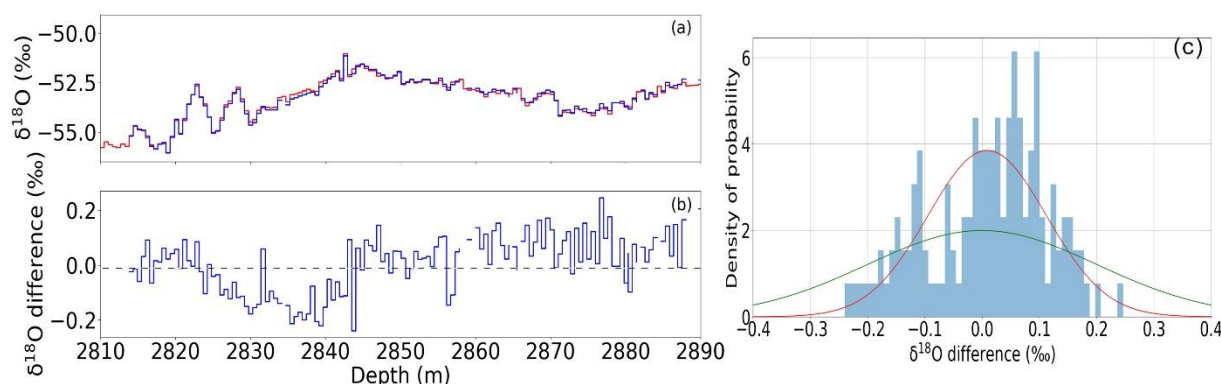
**Table 3: Time resolution of the different MRA decomposition for specific intervals (0-56, 56-144, 144-305, 305-420, 420-651, 651-800 kyrs). Letters a, b, c, d, e and f represent segments that have the same time resolution and can be combined.**

460



465

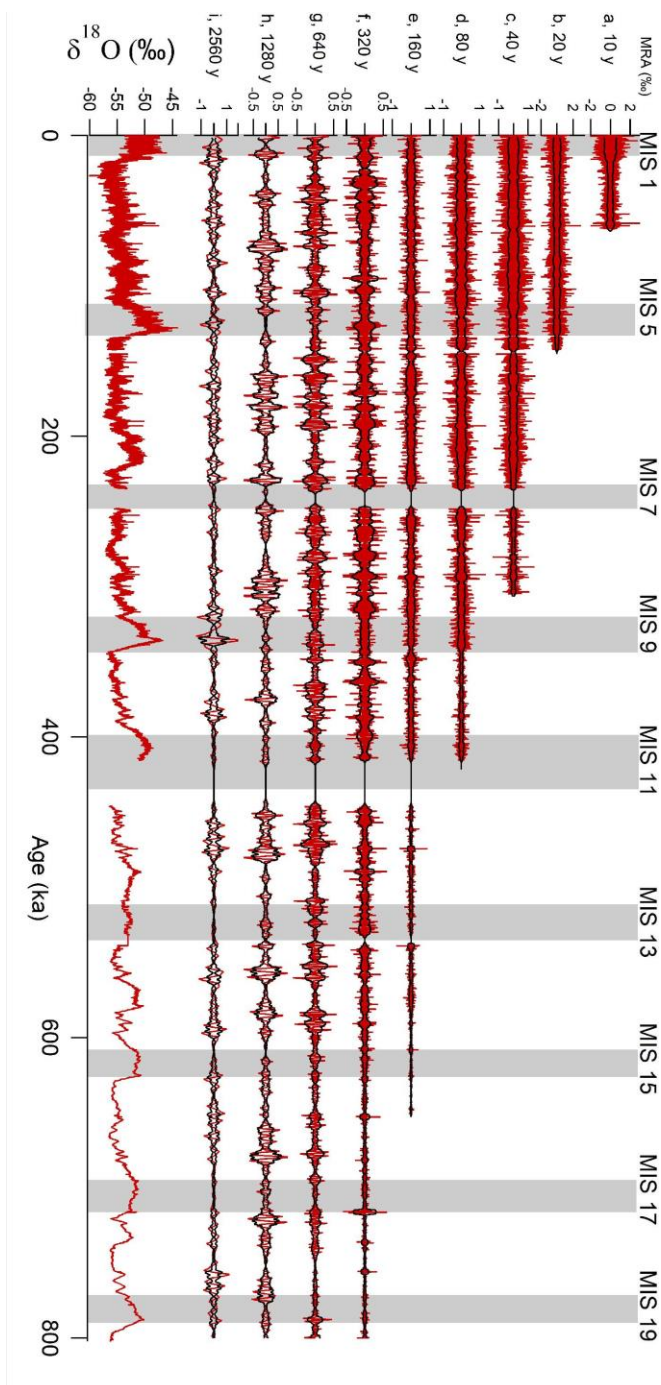
**Figure 2:** (a) Evolution with depth of  $\delta D$  measurements over Termination 2 performed in 2010 at LSCE with the Uranium reduction method (Pol et al., 2014) (blue) and  $\delta D$  measurements performed in 2019 by CRDS at LSCE (red). (b) Difference between the  $\delta D$  values measured in 2010 and 2019. (c) Probability Density Function for the difference between the first (Uranium reduction) and the new (CRDS)  $\delta D$  measurements. A Gaussian curve (red) is fitted to the data. A gaussian curve (green) is displayed with the standard deviation equal to the classically displayed  $1\sigma$  uncertainty of  $\delta D$  measurements with CRDS method at LSCE ( $1\sigma = 0.7$  ‰).



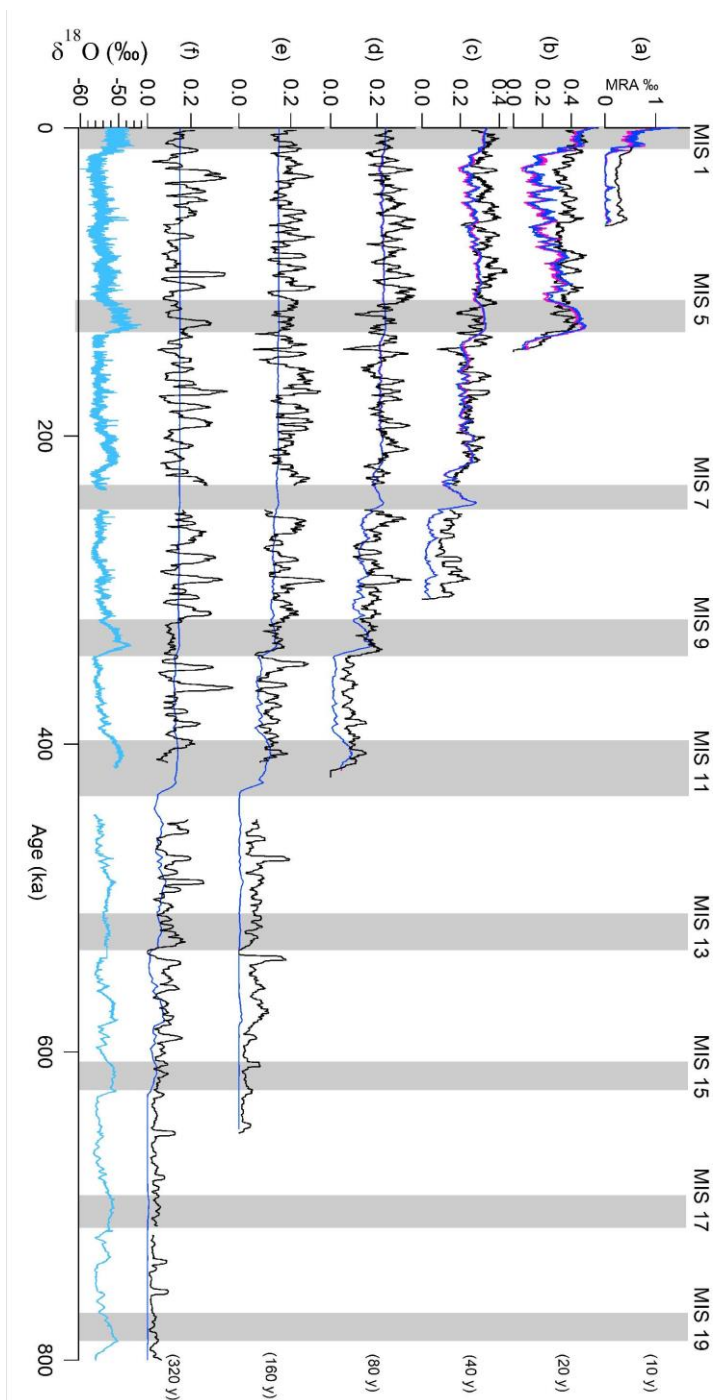
470

**Figure 3:** (a) Evolution with depth of  $\delta^{18}O$  measurements over Termination 6 performed in 2010 at the University of Trieste with  $CO_2$  equilibration method (blue) and  $\delta^{18}O$  measurements performed in 2019 by CRDS at LSCE (red). (b) Difference between the  $\delta^{18}O$  values measured in 2010 and 2019. (c) Probability Density Function for the difference between the old (University of Trieste) and the new (LSCE)  $\delta^{18}O$  measurements. A gaussian curve (red) is fitted to the data. A gaussian curve (green) is displayed with the standard deviation equal to the classically displayed  $1\sigma$  uncertainty of  $\delta^{18}O$  measurements by CRDS at LSCE ( $1\sigma = 0.2$  ‰).

475



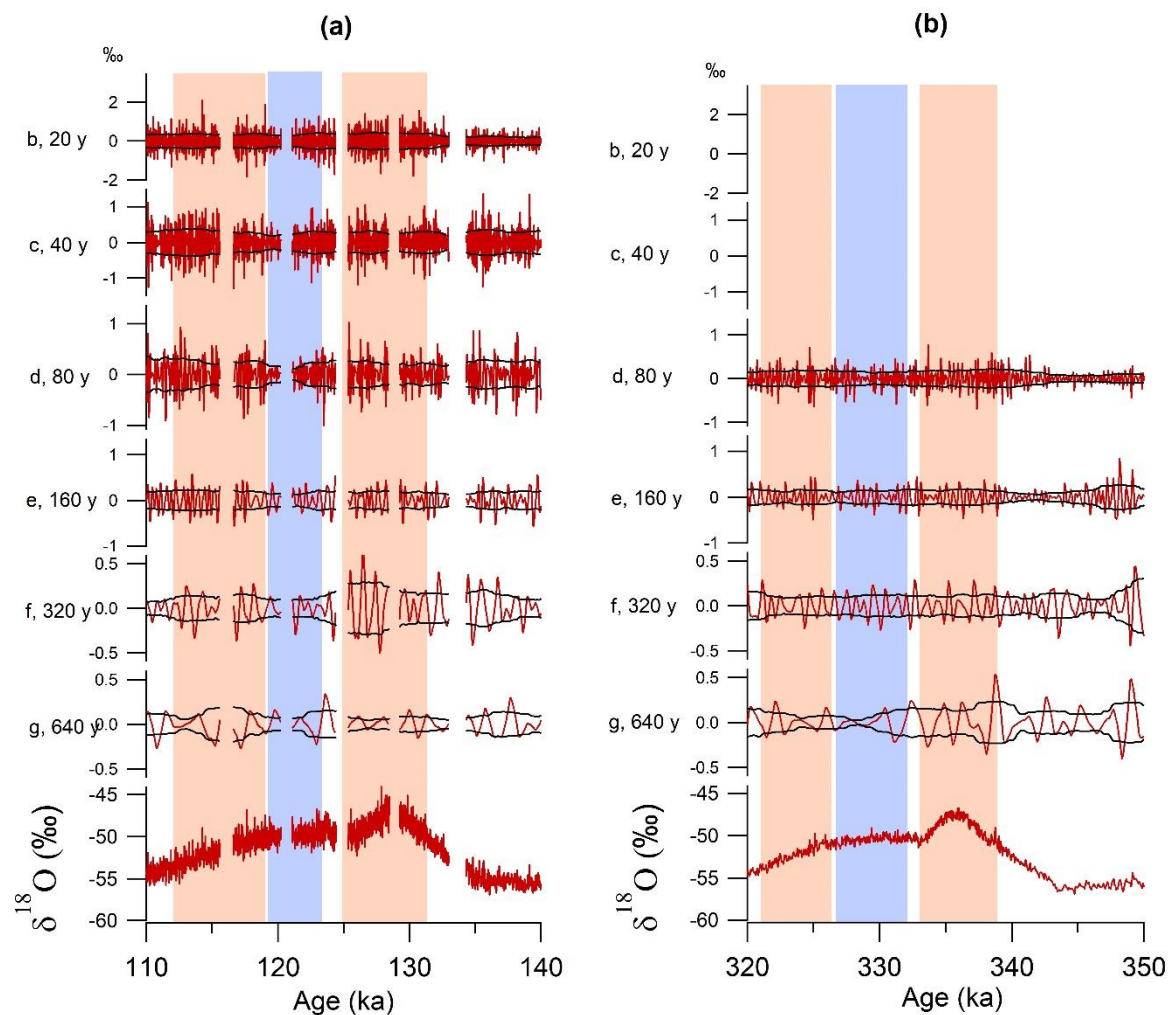
480 **Figure 4: Contribution to the original  $\delta^{18}\text{O}$  signal (red) of the MRA composites of resolution 10 (a), 20 (b), 40 (c), 80 (d), 160 (e), 320 (f), 640 (g), 1280 (h) and 2560 years (i). Marine Isotope Stage intervals are marked in grey bars. The black envelop presents the running standard deviation ( $1\sigma$ ) on 3 kyr windows.**



485 **Figure 5: High resolution record (light blue) and comparison of its variability (3 kyr standard deviation, black) to the variability (3 kyr standard deviation) of the diffused Holocene signal for the different periods (10, 20, 40, 80, 160, 320 years for panels (a) to (f)). The diffused Holocene signal has been calculated using two  $\sigma_{fm}$  estimates, one constant  $\sigma_{fm}$  of 7 cm (dark blue), and one variable  $\sigma_{fm}$  equal to 6.5 cm in glacial period and 7.5 cm in interglacial period (pink).**



490



495

**Figure 6: Contribution to the original  $\delta^{18}\text{O}$  signal (red) of the MRA composites of resolution 20 (b), 40 (c), 80 (d), 160 (e), 320 (f) and 640 (g) years (i) for MIS 5 (left - a) and MIS 9 (right - b). The black envelop presents the running standard deviation ( $1\sigma$ ) on 3 kyr windows. The red rectangles indicate periods with enhanced variability and the blue rectangles indicate periods with reduced variability.**